E-ISSN: 2829-7687

Journal of Fibers and Polymer Composites

Vol. 5 No. 3 (2026): 233-251

Cellulose Nanofiber-Reinforced PVA Films Incorporated with *Moringa oleifera* Leaf Extract: Mechanical, UV-Shielding, and Structural Properties

Kadriadi [a] *, Agus Salim Opu [b], Kadex Widhy Wirakusuma [a], Kamaruddin [a], Jefry Jamel [c], Jeri Ariksa [c,d], Angga Bahri Pratama [e], Muhammad Adlan Azka [f]

[a] Department of Mechanical Maintenance Engineering, Politeknik Industri Logam Morowali, Morowali, Indonesia
[b] Department of Mineral Chemical Engineering, Politeknik Industri Logam Morowali, Morowali, Indonesia
[c] Department of Mechanical Engineering, Universitas Andalas, Padang, Indonesia
[d] Department of Mechanical Engineering, Universitas Bangka Belitung, Bangka, Indonesia
[e] Department of Mechanical Engineering, Politeknik Negeri Medan, Medan, Indonesia
[f] Bioresource Technology Division, School of Industrial Technology, Universiti Sains Malaysia, Penang, Malaysia

Abstract. *Polymer films that combine mechanical durability with ultraviolet (UV) protection are needed for sustainable packaging. In this study, polyvinyl alcohol (PVA) films reinforced with cellulose nanofibers (CNF) and incorporated with Moringa oleifera leaf extract (MLE) were prepared by solution casting at combined loadings of 1–4 wt% CNF and 0.5–2 wt% MLE. The tensile properties, UV–visible transmittance, and crystalline structure of the films were evaluated, and the tensile data were analyzed by one-way ANOVA followed by Duncan's multiple range test ($p < 0.05$). Tensile strength and tensile modulus increased significantly with increasing CNF–MLE loading. The P-CNF4/MLE2 film exhibited the highest tensile strength (75.47 ± 2.89 MPa) and tensile modulus (654.04 ± 14.96 MPa), corresponding to increases of 118.4% and 116.8%, respectively, relative to neat PVA. Although elongation at break decreased at the lowest loading, both elongation at break and toughness increased at higher loadings, reaching 334.43 ± 6.90% and 227.96 ± 15.43 MJ m^{-3}, respectively, for P-CNF4/MLE2. All composite films strongly attenuated UV radiation; films containing at least 2 wt% CNF and 1 wt% MLE transmitted less than approximately 1% of the incident light across the 200–400 nm range, whereas visible-light transmittance at 600 nm decreased from approximately 92% for neat PVA to 45% for P-CNF4/MLE2. X-ray diffraction confirmed that the semicrystalline structure of PVA was retained without the formation of a new crystalline phase, while the crystallinity index increased from 71.79% to 87.91%. The combined incorporation of CNF and MLE therefore produced strong, tough, and UV-shielding PVA films with potential application as light-protective packaging materials.*

Keywords: *Polyvinyl alcohol; Cellulose nanofibers; Moringa oleifera leaf extract; Mechanical properties; UV shielding.*

Type of the Paper: Regular Article.

1. Introduction

The widespread reliance on petroleum-derived plastics for food packaging has become a major environmental problem, as these materials are consumed in large quantities, degrade very

https://doi.org/10.55043/jfpc.v5i3.728
Received September 30, 2026; Received in revised form October 6, 2026; Accepted October 7, 2026; Published October 30, 2026
* Corresponding author
Email: dkadriadi@gmail.com *
© 2026 The Authors. Published by Green Engineering Society on Journal of Fibers and Polymer Composites
This is an open access article under the CC BY-SA 4.0 license https://creativecommons.org/licenses/by-sa/4.0

slowly, and accumulate persistently in terrestrial and marine environments [1]. Conventional plastics nevertheless continue to dominate the market owing to their low cost, easy processability, durability, and effective protection of packaged goods from the surrounding environment. Any sustainable substitute must therefore offer sufficient mechanical integrity and functional performance throughout processing, storage, distribution, and use [2]. In addition to acting as physical barriers, packaging materials are now increasingly required to shield their contents from ultraviolet (UV) radiation, which accelerates the deterioration of light-sensitive products [3].

Polyvinyl alcohol (PVA) is widely studied as a matrix for sustainable packaging films, owing to its good film-forming capacity, high optical clarity, flexibility, adequate mechanical properties, and compatibility with solution casting [4–6]. It is water-soluble, biodegradable under suitable environmental conditions, and rich in hydroxyl groups that readily interact with polysaccharides, nanocellulose, and plant-derived compounds [7,8]. Moreover, PVA exhibits relatively low oxygen permeability under dry conditions, making it potentially suitable for packaging oxidation-sensitive products. However, neat PVA films have important limitations, including high hydrophilicity, moisture sensitivity, and inadequate UV-shielding performance [9]. Because PVA contains abundant hydroxyl groups, it readily absorbs water from humid surroundings; the absorbed water plasticizes the polymer, disrupts its crystalline domains, and markedly increases gas permeability, so the excellent oxygen barrier of dry PVA deteriorates considerably at high relative humidity [10]. In practice, this moisture sensitivity can cause swelling, dimensional instability, loss of mechanical strength, and reduced barrier protection when PVA films are in contact with moist foods or are stored and distributed under humid conditions, such as those typical of tropical climates and refrigerated supply chains [9,10]. Furthermore, neat PVA is highly transparent and transmits a large fraction of UV-A and part of the UV-B radiation; it therefore offers little protection against UV-induced lipid photo-oxidation, vitamin and pigment degradation, discoloration, and off-flavor development in light-sensitive products such as dairy products, oils, meat, and fresh produce [3]. Overcoming these limitations is thus essential if PVA films are to move beyond dry-goods applications and serve as protective packaging for perishable and photosensitive foods. In addition, their balance of strength, stiffness, and extensibility may be insufficient for demanding packaging applications [11]. These limitations have encouraged the incorporation of renewable reinforcing and functional materials into PVA matrices.

Cellulose nanofibers (CNFs) are attractive renewable reinforcing agents for packaging films because they combine a high aspect ratio, high specific strength and stiffness, low density, biodegradability, and surfaces rich in hydroxyl groups [12,13]. Hydrogen bonding between CNF

and PVA favors interfacial compatibility, and well-dispersed CNFs can restrict the mobility of PVA chains and form a reinforcing network that facilitates stress transfer from the polymer matrix to the nanofibers [14,15]. Consequently, CNF incorporation can improve tensile strength, tensile modulus, toughness, and structural integrity. CNF may also influence the molecular arrangement and crystallization behavior of PVA chains, which can be examined using X-ray diffraction.

How effectively CNF reinforces a polymer is governed largely by its content, its state of dispersion, and its interaction with the matrix. At a suitable content, CNF enhances interfacial load transfer and mechanical stability; however, excessive loading or poor dispersion leads to nanofiber agglomeration and stress-concentration sites, which can lower extensibility and trigger premature failure [16]. Therefore, tensile strength alone is insufficient to describe the overall mechanical performance of PVA/CNF films. A more comprehensive evaluation should include the stress–strain response, tensile modulus, elongation at break, and toughness, particularly because packaging films must withstand both tensile loading and deformation during handling and use [17].

Although CNF can improve the structural and mechanical performance of PVA films, an additional functional component is required to enhance protection against UV radiation. Plant extracts are appealing for this purpose because their natural constituents can interact with polymer networks and simultaneously impart optical or biological functions. *Moringa oleifera* leaves contain phenolic acids, flavonoids, tannins, pigments, and other secondary metabolites [18]. Compounds such as quercetin, kaempferol, and caffeoylquinic acid derivatives have been identified in *M. oleifera* leaves [18]. The conjugated structures and chromophoric groups of these phytochemicals can absorb radiation in the UV region, suggesting that Moringa leaf extract (MLE) may serve as a natural UV-shielding component in polymer films.

In food packaging, UV protection matters because UV exposure accelerates photo-oxidation, pigment breakdown, nutrient loss, and undesirable color changes, particularly in oxidation-sensitive products. Incorporating plant-derived UV absorbers into PVA films may reduce UV transmission without relying entirely on synthetic UV-blocking agents [19,20]. However, the pigments and phenolic compounds present in plant extracts may also reduce visible-light transparency and alter the molecular organization of the polymer matrix [21]. Therefore, formulation design must balance UV-shielding performance with optical transparency, strength, stiffness, extensibility, and toughness.

The phenolic hydroxyl groups of MLE constituents may form hydrogen bonds with the hydroxyl groups of PVA and CNF. Such interactions may modify polymer-chain packing, molecular cohesion, and interfacial adhesion within the composite film [22,23]. At the same

time, low-molecular-weight extract constituents may increase free volume or facilitate local chain rearrangement, potentially influencing film extensibility [24,25]. On the other hand, poor compatibility or uneven distribution of the extract may create structural heterogeneity. The final properties of PVA/CNF/MLE films are therefore expected to depend on the balance among CNF reinforcement, molecular interactions, extract distribution, and changes in polymer-chain organization [26].

Previous studies have demonstrated the reinforcement of PVA films using nanocellulose and the functionalization of polymeric or biopolymer films using plant-derived extracts [27,28]. MLE has also been incorporated into different film-forming matrices to provide antioxidant, antimicrobial, or light-barrier functionality. For example, Buasri et al. loaded moringa and guava leaf extracts into PVA/graphene oxide films for food packaging [29], Mohamad et al. blended moringa leaves and MgO nanoparticles into chitosan-based films for active food packaging [30], and Bhat et al. incorporated Moringa extract into chitosan/guar gum/PVA films for food packaging applications [31]. However, in these systems MLE was not combined with a nanocellulose reinforcement, and studies on the combined incorporation of CNF and MLE into a PVA matrix remain limited. In particular, the relationship between the combined CNF–MLE loading and the mechanical, optical, and structural characteristics of PVA films has not been sufficiently clarified. A simultaneous evaluation of stress–strain behavior, tensile strength, tensile modulus, elongation at break, toughness, UV transmittance, and crystalline organization is therefore required to establish whether this combined formulation can provide both mechanical durability and effective UV protection.

Accordingly, this study aimed to develop PVA films containing combined CNF and MLE loadings and to evaluate their mechanical, UV-shielding, and structural properties. Four composite formulations containing 1–4 wt% CNF and 0.5–2 wt% MLE were investigated. The mechanical properties of the films were characterized in terms of stress–strain curves, tensile strength, tensile modulus, elongation at break, and toughness. UV-shielding and visible-light transmittance were evaluated using UV–visible spectroscopy, while changes in molecular ordering and crystalline structure were examined using X-ray diffraction. The relationships among the combined CNF–MLE loading, mechanical performance, optical transmittance, and structural characteristics were then analyzed to assess the potential of these films as mechanically robust, light-protective packaging materials.

2. Materials and Methods

2.1 Materials

Polyvinyl alcohol (PVA), with a molecular weight of 89,000–98,000 g mol^{-1} and a degree

of hydrolysis of 99%, was purchased from Sigma-Aldrich Pte. Ltd. (Singapore). Cellulose nanofibers (CNF) were purchased from Nanografi Nano Technology (Ankara, Türkiye). Fresh *Moringa oleifera* leaves were collected in Kendari, Southeast Sulawesi, Indonesia. Ethanol (96%), used as the extraction solvent, was supplied by the Laboratory of Mineral Chemical Engineering, Politeknik Industri Logam Morowali (Morowali, Indonesia). All solutions, dispersions, and film-forming mixtures were prepared with distilled water, and all reagents were used as supplied without additional purification.

2.2 Preparation of Moringa oleifera Leaf Extract

Fresh *M. oleifera* leaves were dried in air at room temperature until their mass remained constant and were then milled into a fine powder with a laboratory mill (Polymix PX-MFC 90D, Kinematica AG, Switzerland). The extract was prepared by cold maceration: 500 g of leaf powder was immersed in 2 L of 96% ethanol (solid-to-solvent ratio of 1:4, w/v) and agitated continuously on an orbital shaker for 72 h at room temperature. To limit solvent loss and the photodegradation of phytochemicals, the vessel was kept tightly closed and shielded from light throughout maceration. The mixture was then filtered through Whatman filter paper, and the filtrate was concentrated under reduced pressure using a rotary evaporator at 40 °C. The concentrate was subsequently left to dry at room temperature, and the resulting dry extract was kept in tightly closed tubes at 4 °C until further use. The extraction yield, calculated as the mass of dry extract relative to the mass of dry leaf powder, was 11.7 ± 0.4% (w/w). Before being added to the film-forming mixture, the dry extract was redissolved in distilled water at the required concentration; the extract dissolved completely, and no insoluble residue was observed.

2.3 Preparation of the Cellulose Nanofiber Dispersion

Commercial CNF was used without further isolation or chemical treatment. A weighed quantity of CNF was suspended in distilled water, stirred magnetically at 500 rpm for 60 min at room temperature, and subsequently treated with a high-shear homogenizer at 10,000 rpm for 5 min to obtain a uniform dispersion with minimal nanofiber agglomeration. The resulting dispersion was kept in a closed container and homogenized again just before it was mixed with the PVA solution.

2.4 Preparation of PVA/CNF/Moringa Leaf Extract Films

The PVA/CNF/MLE films were fabricated by solution casting, using a procedure modified from earlier work on PVA films containing cellulose nanofibers or plant extracts [14,19]. All compositions were expressed relative to the total dry-solid mass of PVA, CNF, and MLE (Table 1). Five formulations were produced, namely neat PVA and four composites containing 1–4 wt%

CNF and 0.5–2 wt% MLE, in which the PVA fraction was adjusted so that the total solid content equaled 100 wt%. The total solid concentration of each film-forming solution was kept constant at 10 g per 100 mL of distilled water (10% w/v); the absolute masses of PVA, CNF, and MLE in each formulation can therefore be obtained by multiplying this value by the weight fractions given in Table 1 (e.g., 9.4 g of PVA, 0.4 g of CNF, and 0.2 g of MLE for P-CNF4/MLE2). For each formulation, PVA was dissolved in 100 mL of distilled water at 80 °C for 2 h under continuous magnetic stirring at 500 rpm (Scilogex MS-H280-Pro) until a clear, homogeneous solution formed. The solution was subsequently sonicated with an ultrasonic processor (SJIA-1200W) at 360 W for 5 min. The required amount of the CNF dispersion was gradually added to the PVA solution at approximately 80 °C, and the mixture was stirred at 500 rpm for 10 min to distribute the CNF uniformly throughout the polymer matrix.

The PVA/CNF mixture was then cooled to approximately 50 °C, and the MLE solution was added at the concentration specified for each formulation (Table 1). Stirring was continued at 500 rpm for a further 10 min to distribute the extract and allow it to interact with PVA and CNF, after which the mixture was sonicated again (360 W, 5 min) to reduce CNF agglomeration and improve its homogeneity. The neat PVA film was prepared using the same procedure without the addition of CNF and MLE. Subsequently, 50 mL of each film-forming mixture was cast into a Petri dish (diameter 13 cm) and dried in a vacuum oven at 50 °C for 21 h. The dried films were gently detached from the dishes and visually checked for defects. Before characterization, all films were conditioned at 28 °C and 50 ± 5% relative humidity (RH) for 48 h. The average thicknesses of the resulting films are listed in Table 1.

Table 1. Composition of neat PVA and PVA/CNF/MLE films

Sample Code	PVA (wt%)	CNF (wt%)	MLE (wt%)	Thickness (mm)
PVA	100	0	0	0.21
P-CNF1/MLE0.5	98.5	1	0.5	0.22
P-CNF2/MLE1	97.0	2	1	0.22
P-CNF3/MLE1.5	95.5	3	1.5	0.23
P-CNF4/MLE2	94.0	4	2	0.23

2.5 Characterization

2.5.1 Tensile Properties

Tensile tests were carried out on a universal testing machine (AGS-X, Shimadzu, Japan) according to ASTM D882, the standard method for thin plastic sheeting less than 1 mm thick. Rectangular strip specimens measuring 10 mm × 100 mm were cut from each film and tested at an initial grip separation (gauge length) of 50 mm. Before testing, the specimens were conditioned at 28 °C and 50 ± 5% RH for 48 h, as described in Section 2.4. The thickness and

width of every specimen were determined with a digital micrometer (resolution 0.001 mm). The tests were performed at a crosshead speed of 5 mm min^{-1}. Tensile strength, tensile modulus, and elongation at break were obtained from the stress–strain curves; the tensile modulus was calculated from the slope of the initial linear region, and toughness was calculated as the area under the stress–strain curve. Five specimens of each formulation were tested, and the results are reported as mean ± standard deviation.

2.5.2 UV–Visible Spectroscopy

The optical transmittance and UV-blocking performance of the films were evaluated using a UV–visible spectrophotometer (UV-1800, Shimadzu, Japan) over the wavelength range of 200–800 nm. Film strips (10 mm × 25 mm) were placed directly in the sample holder, with an empty holder (air) serving as the reference. Transmittance was analyzed in the UV-C (200–280 nm), UV-B (280–315 nm), UV-A (315–400 nm), and visible (400–800 nm) regions. Three specimens of each formulation were measured. A lower transmittance between 200 and 400 nm was taken to indicate superior UV-blocking ability, while the visible-region transmittance was used to evaluate how CNF and MLE affected film transparency.

2.5.3 X-Ray Diffraction Analysis

The crystalline structures of the films were examined using an X-ray diffractometer (XRD-7000 Maxima X, Shimadzu Corporation, Japan) with Cu Kα radiation (λ = 0.154 nm) operated at 40 kV and 30 mA. The patterns were collected at 25 °C over a 2θ range of 5–60° with a step size of 0.02° and a scan speed of 2° min^{-1}. The XRD patterns are presented as recorded, without smoothing, background subtraction, or any other signal processing, and the CI was calculated from these unprocessed intensities. The relative crystallinity index (CI) was estimated using the peak-height method [32], as expressed in Eq. (1).

where I_{max} is the maximum intensity of the principal PVA reflection at 2θ ≈ 19.5–20° and I_{am} is the intensity of the amorphous region. Because the CI was calculated from peak intensities, it was used as a relative index to compare the formulations rather than as an absolute degree of crystallinity.

2.5.4 Statistical Analysis

Tensile strength, tensile modulus, elongation at break, and toughness were analyzed by one-way analysis of variance (ANOVA) to determine the effect of film formulation. When a significant effect was detected, Duncan's multiple range test was used as a post hoc test to compare the formulations. Differences were considered statistically significant at $p < 0.05$.

3. Results and Discussion

3.1 Tensile Properties

Figs. 1 and 2 present the tensile properties and representative stress–strain curves of neat PVA and the PVA/CNF/MLE films. Neat PVA exhibited a tensile strength of 34.55 ± 1.25 MPa and a tensile modulus of 301.70 ± 11.31 MPa (Fig. 1a). Both properties increased significantly and progressively with increasing CNF–MLE loading ($p < 0.05$). The tensile strength increased to 40.69 ± 1.53, 47.71 ± 1.69, 65.14 ± 1.42, and 75.47 ± 2.89 MPa for P-CNF1/MLE0.5, P-CNF2/MLE1, P-CNF3/MLE1.5, and P-CNF4/MLE2, respectively, while the tensile modulus increased from 355.00 ± 10.95 MPa for P-CNF1/MLE0.5 to 654.04 ± 14.96 MPa for P-CNF4/MLE2. Different lowercase letters in Fig. 1 denote significant differences among the formulations ($p < 0.05$).

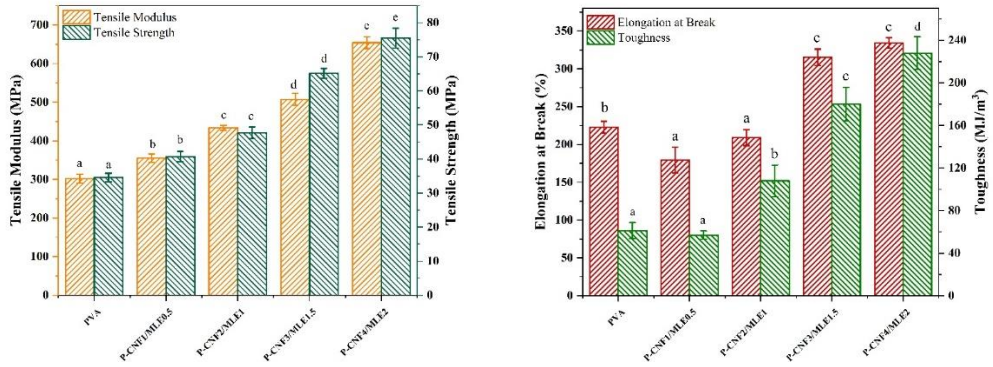


Fig. 1. (a) Tensile modulus and tensile strength and (b) elongation at break and toughness of neat PVA and PVA/CNF/MLE films. Different lowercase letters above the bars of the same property indicate significant differences ($p < 0.05$).

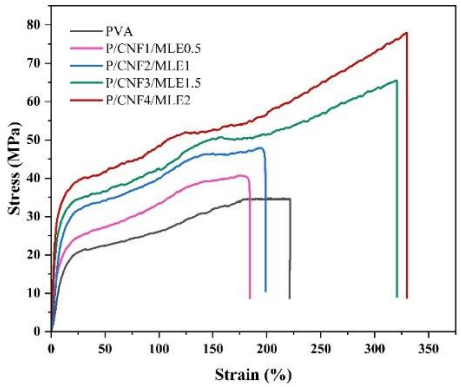


Fig. 2. Representative stress–strain curves of neat PVA and PVA/CNF/MLE films.

Relative to neat PVA, P-CNF4/MLE2 showed increases of 118.4% in tensile strength and 116.8% in tensile modulus, indicating that the combined incorporation of CNF and MLE produced a markedly stronger and stiffer film. CNF is an effective reinforcement because of its

high intrinsic stiffness, large specific surface area, and hydroxyl-rich surface. The surface hydroxyl groups of CNF can form hydrogen bonds with those of PVA, thereby improving interfacial adhesion and promoting stress transfer from the matrix to the nanofibers [14,16,33,34]. The hydroxyl-bearing phenolic constituents of MLE may further contribute to intermolecular interactions with PVA and CNF [19,27,31]. Together, these interactions restrict the mobility of PVA chains and increase the stress required to deform and fracture the films.

The representative stress–strain curves (Fig. 2) are consistent with these results. All films exhibited ductile behavior, with an initial linear elastic region followed by yielding and extensive plastic deformation. With increasing CNF–MLE loading, the curves shifted toward higher stress levels, and the composite films, particularly P-CNF3/MLE1.5 and P-CNF4/MLE2, showed a continuous rise in stress during plastic deformation, which may reflect the progressive alignment of PVA chains and CNF in the loading direction. P-CNF4/MLE2 sustained the highest stress before fracture, followed by P-CNF3/MLE1.5, whereas neat PVA showed the lowest fracture stress. The continuous improvement up to the highest loading suggests that severe CNF agglomeration did not occur within the investigated composition range. However, morphological analysis (e.g., scanning electron microscopy) would be required to confirm the distribution of CNF and MLE in the PVA matrix.

In contrast to tensile strength and modulus, elongation at break followed a non-monotonic trend (Fig. 1b). Neat PVA exhibited an elongation at break of 222.97 ± 7.83%, which decreased significantly to 179.43 ± 16.94% for P-CNF1/MLE0.5, probably because the initial addition of CNF and MLE restricted the mobility of PVA chains. Elongation at break then increased to 209.10 ± 10.56, 315.10 ± 11.00, and 334.43 ± 6.90% for P-CNF2/MLE1, P-CNF3/MLE1.5, and P-CNF4/MLE2, respectively. The value for P-CNF2/MLE1 was not significantly different from that for P-CNF1/MLE0.5, whereas P-CNF3/MLE1.5 and P-CNF4/MLE2 were both significantly more extensible than neat PVA. The elongation at break of P-CNF4/MLE2 was 50.0% higher than that of neat PVA, although it did not differ significantly from that of P-CNF3/MLE1.5.

The recovery and subsequent increase in elongation at higher loadings suggest a shift in the balance between chain restriction and chain mobility. Low-molecular-weight constituents of MLE may act as plasticizers, increasing the free volume between PVA chains and allowing greater molecular rearrangement during deformation [25,35,36]. Meanwhile, a sufficiently interconnected CNF network may maintain structural integrity and delay crack propagation. This interpretation is consistent with the simultaneous increase in tensile strength and elongation at break observed for P-CNF3/MLE1.5 and P-CNF4/MLE2. Nevertheless, morphological and molecular-level characterization (e.g., SEM and FTIR) is needed to confirm this mechanism.

Toughness, calculated as the area under the stress–strain curve, decreased slightly from

61.20 ± 7.40 MJ m^{-3} for neat PVA to 56.92 ± 3.90 MJ m^{-3} for P-CNF1/MLE0.5, although this difference was not statistically significant. At higher loadings, toughness increased significantly to 107.86 ± 14.97, 179.93 ± 15.72, and 227.96 ± 15.43 MJ m^{-3} for P-CNF2/MLE1, P-CNF3/MLE1.5, and P-CNF4/MLE2, respectively. The toughness of P-CNF4/MLE2 was therefore 272.5% higher (approximately 3.7-fold) than that of neat PVA. This improvement arose from the simultaneous increase in tensile strength and strain at break, which enabled the film to absorb substantially more energy before failure [37,38].

Overall, P-CNF4/MLE2 exhibited the best tensile performance among the investigated formulations, with the highest tensile strength, tensile modulus, and toughness, and the highest mean elongation at break. This combination of strength, stiffness, extensibility, and energy absorption is desirable for flexible packaging films that must withstand mechanical stresses during processing, handling, storage, and transportation. However, because the CNF and MLE contents were varied simultaneously, their individual contributions cannot be separated in the present design; the observed changes therefore reflect the combined effect of both components.

3.2 UV–Visible Transmittance

Fig. 3 shows the UV–visible transmittance spectra of neat PVA and the PVA/CNF/MLE films over the range of 200–800 nm. Neat PVA provided limited UV protection: its transmittance rose sharply at approximately 265 nm, remained at approximately 27–38% between 280 and 340 nm, and increased further across the UV-A region to approximately 80% at 400 nm. Thus, neat PVA transmitted a substantial proportion of UV radiation, particularly in the UV-A region. The spectrum of neat PVA also showed a local transmittance maximum of approximately 38% at about 305 nm in the UV-B region, located between two weak absorption features near 280 nm and 330–340 nm. This apparent peak does not indicate that the film structure enhances UV-B transmission; rather, it arises from the intrinsic absorption of PVA on either side of this wavelength. Commercial PVA contains small amounts of carbonyl groups conjugated with ethylenic unsaturation, $–(CH=CH)_n–CO–$, which are introduced during the polymerization of vinyl acetate and the subsequent hydrolysis and thermal processing, together with residual acetate groups. These chromophores absorb at approximately 280 nm (n = 2) and 330 nm (n = 3) [39]. Because they are present only at low concentrations, transmittance partially recovers between the two absorption bands, producing the apparent maximum at approximately 305 nm. The abrupt discontinuities in the neat PVA spectrum near 310 and 340–365 nm may additionally include an instrumental contribution, because light-source and filter changeovers of double-beam spectrophotometers typically occur in this wavelength region. In the composite films, this feature was no longer visible, as the much stronger and broader absorption of MLE

chromophores masked the weak intrinsic absorption of PVA.

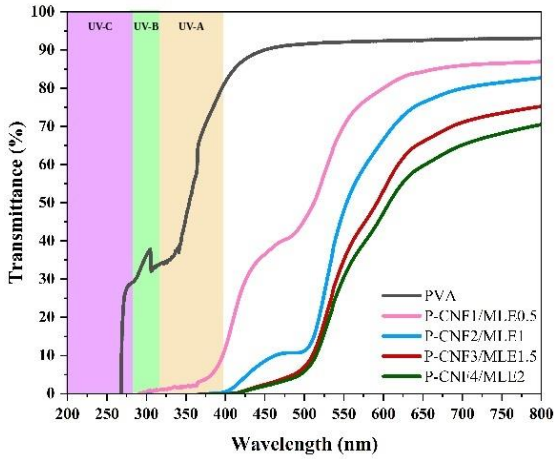


Fig. 3. UV–visible transmittance spectra of neat PVA and PVA/CNF/MLE films over the range of 200–800 nm. The shaded areas indicate the UV-C, UV-B, and UV-A regions.

The combined incorporation of CNF and MLE markedly reduced UV transmittance, consistent with previous reports on polymer films containing plant-derived polyphenolic extracts [31,36]. Even at the lowest loading, P-CNF1/MLE0.5 showed a transmittance of essentially 0% in the UV-C region and below approximately 1% in the UV-B region; its transmittance remained below approximately 3% up to 370 nm and then increased steeply in the upper UV-A region to approximately 10% of the incident light at 400 nm. Higher loadings further improved UV shielding: P-CNF2/MLE1, P-CNF3/MLE1.5, and P-CNF4/MLE2 showed transmittance below approximately 1% across the entire 200–400 nm range, indicating almost complete blocking of UV-C, UV-B, and UV-A radiation. Because the transmittance of these three films remained below 1%, only minor differences among them were observed in the UV region.

The enhanced UV-shielding performance can be attributed mainly to the UV-absorbing constituents of MLE. Moringa leaves contain phenolic acids, flavonoids, tannins, chlorophylls, carotenoids, and other compounds with conjugated chromophores that absorb UV radiation through $\pi \rightarrow \pi^*$ and $n \rightarrow \pi^*$ electronic transitions [3,40]. CNF may also contribute by scattering incident light and modifying the internal structure of the films [13,41]. However, because the CNF and MLE contents were increased simultaneously, their individual contributions to UV attenuation cannot be quantified using the present formulation design.

The incorporation of CNF and MLE also reduced transmittance in the visible region. At 600 nm, neat PVA exhibited a transmittance of approximately 92%, confirming its high optical transparency, whereas P-CNF1/MLE0.5, P-CNF2/MLE1, P-CNF3/MLE1.5, and P-CNF4/MLE2 transmitted approximately 80, 65, 52, and 45%, respectively. At 800 nm, the corresponding values for neat PVA and the four composite films were approximately 93, 87, 83, 75, and 70%.

This reduction likely resulted from the combined effects of light absorption and light scattering, as previously reported for PVA films containing nanocellulose and/or plant-derived extracts [13,16,27,42]. The low transmittance of the composite films in the 400–500 nm region is consistent with absorption by MLE pigments, such as chlorophylls and carotenoids, and by polyphenolic compounds, whose concentration in the matrix increased with increasing MLE content [27,36]. Meanwhile, the growing number of CNF–PVA interfaces, the refractive-index mismatch between cellulose and PVA, and possible CNF bundles or structural irregularities may have promoted light scattering, which also reduces the fraction of light transmitted through the film [13,16]. Because the film thickness varied only slightly among the formulations (0.21–0.23 mm; Table 1), the progressive decrease in transmittance from P-CNF1/MLE0.5 to P-CNF4/MLE2 can be attributed mainly to these composition-dependent absorption and scattering effects rather than to differences in optical path length.

The reduction in visible-light transmittance is also evident in the appearance of the films (Fig. 4). Neat PVA was colorless and highly transparent, allowing the printed logo beneath it to be seen clearly. By contrast, the composite films exhibited a yellow to amber coloration that became progressively deeper with increasing CNF–MLE loading, from light yellow for P-CNF1/MLE0.5 to dark amber for P-CNF4/MLE2. This coloration is consistent with the absorption of blue light by MLE pigments and phenolic compounds, in agreement with the low transmittance of the composite films in the 400–500 nm region (Fig. 3). Nevertheless, the printed logo remained legible through all composite films, including P-CNF4/MLE2, indicating that the films retained adequate see-through transparency for product visibility while providing strong UV shielding.



(a) PVA (b) P-CNF1/MLE0.5 (c) P-CNF2/MLE1 (d) P-CNF3/MLE1.5 (e) P-CNF4/MLE2

Fig. 4. Photographs of (a) neat PVA, (b) P-CNF1/MLE0.5, (c) P-CNF2/MLE1, (d) P-CNF3/MLE1.5, and (e) P-CNF4/MLE2 films placed over a printed logo, showing their visual transparency and coloration.

Reduced visible-light transmission may benefit the packaging of foods susceptible to photo-oxidation, discoloration, pigment degradation, or nutrient loss during storage, but lower transparency may be undesirable when clear product visibility is required. The formulation should therefore be selected according to the intended packaging application. Among the

investigated films, P-CNF4/MLE2 combined a UV transmittance below approximately 1% with the lowest visible-light transmittance, providing the strongest overall light-barrier performance. Together with its superior tensile properties, this formulation offered the most favorable balance between mechanical performance and light protection, supporting its potential use as a light-protective packaging film for photosensitive products. Nevertheless, classifying these films as active packaging materials would require experimental verification of active functions, such as antioxidant or antimicrobial activity.

3.3 XRD Analysis

Fig. 5 shows the XRD patterns of neat PVA and the PVA/CNF/MLE films. All films exhibited a broad principal reflection at $2\theta \approx 20°$, together with a weaker reflection at approximately 41°. These reflections are characteristic of semicrystalline PVA, in which ordered crystalline domains coexist with an amorphous phase [4,14,43]. After the incorporation of CNF and MLE, the position of the principal peak remained essentially unchanged and no new peaks appeared, indicating that the semicrystalline structure of PVA was retained without the formation of a detectable separate crystalline phase. The absence of distinct cellulose I reflections (typically at $2\theta \approx 16°$ and 22.5°) can be attributed to the low CNF content and the overlap of these reflections with the broad PVA peak. Similar retention of the characteristic PVA reflection has been reported for nanocellulose-reinforced PVA films [16]. However, the intensity of the principal reflection increased progressively in the order PVA < P-CNF1/MLE0.5 < P-CNF2/MLE1 < P-CNF3/MLE1.5 < P-CNF4/MLE2. Consistently, the CI increased from 71.79% for neat PVA to 72.72, 85.20, 85.33, and 87.91% for P-CNF1/MLE0.5, P-CNF2/MLE1, P-CNF3/MLE1.5, and P-CNF4/MLE2, respectively. Because all films had a similar thickness (0.21–0.23 mm), these differences reflect changes in structural order rather than differences in the amount of irradiated material. The CI changed only marginally at the lowest loading but increased sharply to 85.20% for P-CNF2/MLE1, followed by a smaller increase at higher loadings, suggesting that a threshold CNF–MLE content was required to substantially promote chain ordering. These changes indicate a greater contribution from ordered domains, which may be associated with the crystalline domains of CNF and with the improved organization of PVA chains around the reinforcing phase, as CNF can act as a nucleating site for PVA crystallization [33,44].

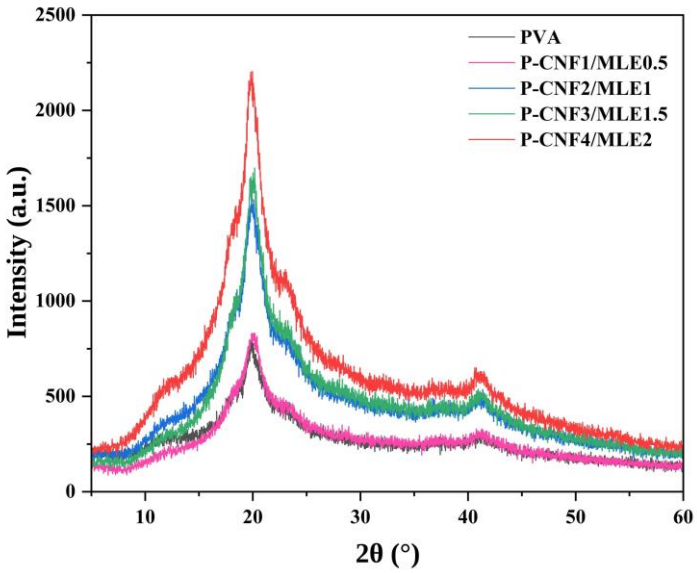


Fig. 5. XRD patterns (raw data, without smoothing) of neat PVA and PVA/CNF/MLE films.

The XRD results are consistent with the tensile properties of the films. The greater contribution of ordered domains, combined with the preserved semicrystalline PVA structure, suggests the formation of a more organized composite matrix that facilitated stress transfer between PVA and CNF. Previous studies have likewise shown that nanocellulose can enhance the structural ordering, interfacial interactions, tensile strength, and stiffness of PVA films [45]. In the present study, the increase in CI generally paralleled the increases in tensile strength and tensile modulus, and P-CNF4/MLE2, which showed the highest CI (87.91%), also exhibited the highest tensile strength (75.47 MPa) and tensile modulus (654.04 MPa). Notably, the sharp increase in CI at P-CNF2/MLE1 coincided with the onset of a significant increase in toughness, whereas the marginal CI change for P-CNF1/MLE0.5 was accompanied by no significant change in toughness. However, the CI of P-CNF2/MLE1 and P-CNF3/MLE1.5 was nearly identical (85.20 and 85.33%), whereas the tensile strength of P-CNF3/MLE1.5 was 36.5% higher, indicating that crystalline ordering alone cannot account for the reinforcement and that CNF load transfer and interfacial interactions also contributed [37]. Because increased crystalline order is generally associated with reduced extensibility, the concurrent increase in elongation at break at higher loadings suggests that MLE constituents plasticized the amorphous regions of PVA, while the ordered domains and the CNF network supported load bearing. Overall, the XRD results indicate that the incorporation of CNF and MLE preserved the semicrystalline structure of PVA while increasing structural ordering, which supports the mechanical reinforcement of the composite films.

4. Conclusions

PVA films reinforced with CNF and incorporated with MLE were successfully prepared by solution casting at combined loadings of 1–4 wt% CNF and 0.5–2 wt% MLE. Increasing the CNF–MLE loading significantly improved the tensile strength and tensile modulus, which reached 75.47 and 654.04 MPa, respectively, for P-CNF4/MLE2, corresponding to increases of 118.4% and 116.8% over neat PVA. Although the lowest loading reduced elongation at break, higher loadings increased extensibility and toughness simultaneously, with P-CNF4/MLE2 reaching an elongation at break of 334.43% and a toughness of 227.96 MJ m^{-3}. The incorporation of CNF and MLE converted the UV-transmitting PVA film into an effective UV barrier: films containing at least 2 wt% CNF and 1 wt% MLE transmitted less than approximately 1% of the incident light in the 200–400 nm range, at the cost of reduced visible-light transparency. XRD analysis showed that the semicrystalline structure of PVA was preserved, while the crystallinity index increased from 71.79% to 87.91%, consistent with the observed mechanical reinforcement. These findings demonstrate that combining a nanocellulose reinforcement with a plant-derived UV absorber is a simple route to strong, tough, and UV-shielding PVA films, with P-CNF4/MLE2 being the most promising formulation for the light-protective packaging of photosensitive products.

Because CNF and MLE were varied simultaneously in this study, future work should use a factorial design to separate their individual contributions. Further studies should also examine film morphology, chemical interactions (FTIR), thermal stability, water resistance, water vapor and oxygen barrier properties, antioxidant and antimicrobial activity, the migration of extract constituents, and performance in real food packaging applications.

Data availability statement

The data supporting the findings of this study are available from the corresponding author upon reasonable request.

CRediT authorship contribution statement

Kadriadi: Conceptualization, Methodology, Investigation, Formal analysis, Writing – original draft. **Agus Salim Opu**: Resources. **Kadex Widhy Wirakusuma**: Supervision, Writing – review & editing, Investigation. **Kamaruddin**: Investigation. **Jefry Jamel**: Investigation. **Jeri Ariksa**: Investigation. **Angga Bahri Pratama**: Formal analysis. **Muhammad Adlan Azka**: Writing – review & editing, Investigation.

Declaration of Competing Interest

The authors declare that they have no known competing financial interests or personal relationships that could have appeared to influence the work reported in this paper.

Acknowledgement

The authors thank Politeknik Industri Logam Morowali for providing laboratory facilities for this research.

References

[1] Gaur A, Singhal N, Singh R, Jain R, Singh N, Pant G, et al. Microplastics to Metabolomics: Understanding the environmental and health implications of plastic pollution. Polym Test 2025;150:108918. https://doi.org/10.1016/j.polymertesting.2025.108918.

[2] Yuen CB, Chong HL, Kwok M-H, Ngai T. Natural polymer-based food packaging: paving the way to a greener future – a review. Sustainable Food Technology 2025;3:908–29. https://doi.org/10.1039/D5FB00021A.

[3] Roy S, Ramakrishnan R, Goksen G, Singh S, Łopusiewicz Ł. Recent progress on UV-light barrier food packaging films – a systematic review. Innovative Food Science & Emerging Technologies 2024;91:103550. https://doi.org/10.1016/j.ifset.2023.103550.

[4] Abral H, Atmajaya A, Mahardika M, Hafizulhaq F, Kadriadi, Handayani D, et al. Effect of ultrasonication duration of polyvinyl alcohol (PVA) gel on characterizations of PVA film. Journal of Materials Research and Technology 2020;9:2477–86. https://doi.org/10.1016/j.jmrt.2019.12.078.

[5] Aslam M, Kalyar MA, Raza ZA. Polyvinyl alcohol: A review of research status and use of polyvinyl alcohol based nanocomposites. Polym Eng Sci 2018;58:2119–32. https://doi.org/10.1002/pen.24855.

[6] Wang J, Li Z, Liu J, Wu H, Guo M, Wang W, et al. Synergistic Enhancement of Barrier Performance in Silanized Modified Hemicellulose/PVA Composite Films through Oxalic Acid Crosslinking. Ind Crops Prod 2024;215:118644. https://doi.org/10.1016/j.indcrop.2024.118644.

[7] Gu Y, Wang H, Yuan Y, Zhang C, Wu W, Wang W, et al. Lignin-incorporated PVA/chitosan hydrogels with highly enhanced toughness and rigidity through a non-covalent crosslinking strategy. Chemical Engineering Journal 2026;531:173970. https://doi.org/10.1016/j.cej.2026.173970.

[8] Li J, Sun H, Weng Y. Natural Extracts and Their Applications in Polymer-Based Active Packaging: A Review. Polymers (Basel) 2024;16:625. https://doi.org/10.3390/polym16050625.

[9] Panda PK, Sadeghi K, Seo J. Recent advances in poly (vinyl alcohol)/natural polymer based films for food packaging applications: A review. Food Packag Shelf Life 2022;33:100904. https://doi.org/10.1016/j.fpsl.2022.100904.

[10] Nyflött Å, Meriçer Ç, Minelli M, Moons E, Järnström L, Lestelius M, et al. The influence of moisture content on the polymer structure of polyvinyl alcohol in dispersion barrier coatings and its effect on the mass transport of oxygen. J Coat Technol Res 2017;14:1345–55. https://doi.org/10.1007/s11998-017-9937-2.

[11] Kuchaiyaphum P, Chotichayapong C, Kajsanthia K, Saengsuwan N. Carboxymethyl cellulose/poly (vinyl alcohol) based active film incorporated with tamarind seed coat waste extract for food packaging application. Int J Biol Macromol 2024;255:128203. https://doi.org/10.1016/j.ijbiomac.2023.128203.

[12] Marinho E. Cellulose: A comprehensive review of its properties and applications. Sustainable Chemistry for the Environment 2025;11:100283. https://doi.org/10.1016/j.scenv.2025.100283.

[13] Nguyen S Van, Lee B-K. PVA/CNC/TiO2 nanocomposite for food-packaging: Improved mechanical, UV/water vapor barrier, and antimicrobial properties. Carbohydr Polym 2022;298:120064. https://doi.org/10.1016/j.carbpol.2022.120064.
[14] Abral H, Kadriadi, Mahardika M, Handayani D, Sugiarti E, Muslimin AN. Characterization of disintegrated bacterial cellulose nanofibers/PVA bionanocomposites prepared via ultrasonication. Int J Biol Macromol 2019;135:591–9. https://doi.org/10.1016/j.ijbiomac.2019.05.178.
[15] Rafique HAR, Lee B-K. Bio-derived carbon dot-loaded PVA/CNC films with antioxidant, UV-blocking, and antimicrobial properties for active food packaging. Int J Biol Macromol 2026;337:149455. https://doi.org/10.1016/j.ijbiomac.2025.149455.
[16] Mahardika M, Masruchin N, Amelia D, Ilyas RA, Septevani AA, Syafri E, et al. Nanocellulose reinforced polyvinyl alcohol-based bio-nanocomposite films: improved mechanical, UV-light barrier, and thermal properties. RSC Adv 2024;14:23232–9. https://doi.org/10.1039/D4RA04205K.
[17] Alvarado MC. Recent progress in polyvinyl alcohol (PVA)/nanocellulose composite films for packaging applications: A comprehensive review of the impact on physico-mechanical properties. Food Bioengineering 2024;3:189–209. https://doi.org/10.1002/fbe2.12086.
[18] Leone A, Spada A, Battezzati A, Schiraldi A, Aristil J, Bertoli S. Cultivation, Genetic, Ethnopharmacology, Phytochemistry and Pharmacology of Moringa oleifera Leaves: An Overview. Int J Mol Sci 2015;16:12791–835. https://doi.org/10.3390/ijms160612791.
[19] Kadriadi, Rahmadiawan D, Abral H, Ilhamdi, Ivan M, Akmal, et al. A novel active packaging film based on polyvinyl alcohol/bajakah tampala (Spatholobus littoralis hassk) extract: Enhancing mechanical, UV protection, thermal stability, antimicrobial, and barrier properties. Food Biosci 2025;68:106500. https://doi.org/10.1016/j.fbio.2025.106500.
[20] Kadriadi K, Abral H, Mahardika M, Ilhamdi I, Akmal A, Handayani D, et al. Modified PVA Film from Methanol-Soluble Phenolic Extracts of Spatholobus littoralis Hask as Active Pharmaceutical Packaging. Journal of Fibers and Polymer Composites 2026;5:19–30. https://doi.org/10.55043/jfpc.v5i1.567.
[21] Koopmann A-K, Schuster C, Torres-Rodríguez J, Kain S, Pertl-Obermeyer H, Petutschnigg A, et al. Tannin-Based Hybrid Materials and Their Applications: A Review. Molecules 2020;25:4910. https://doi.org/10.3390/molecules25214910.
[22] Andrade J, González-Martínez C, Chiralt A. Physical and active properties of poly (vinyl alcohol) films with phenolic acids as affected by the processing method. Food Packag Shelf Life 2022;33:100855. https://doi.org/10.1016/j.fpsl.2022.100855.
[23] Osolnik U, Vek V, Korošec RC, Oven P, Poljanšek I. Integration of wood-based components – Cellulose nanofibrils and tannic acid - into a poly(vinyl alcohol) matrix to improve functional properties. Int J Biol Macromol 2024;256:128495. https://doi.org/10.1016/j.ijbiomac.2023.128495.
[24] Zhang S, Zhang X, Wan X, Zhang H, Tian J. Fabrication of biodegradable films with UV-blocking and high-strength properties from spent coffee grounds. Carbohydr Polym 2023;321:121290. https://doi.org/10.1016/j.carbpol.2023.121290.
[25] Carmona-Cantillo D, Gonzalez-Muñoz G, López-Padilla A, Rico-Rodríguez F, Ortega-Toro R. Development of Intelligent Composite Materials from Polyvinyl Alcohol (PVA) and Clitoria ternatea L. Anthocyanin Extract for Shrimp Freshness Monitoring. Polymers (Basel) 2026;18:684. https://doi.org/10.3390/polym18060684.
[26] Nogueira GF, Oliveira RA de, Velasco JI, Fakhouri FM. Methods of Incorporating Plant-Derived Bioactive Compounds into Films Made with Agro-Based Polymers for Application as Food Packaging: A Brief Review. Polymers (Basel) 2020;12:2518. https://doi.org/10.3390/polym12112518.
[27] Sunarsono H, Abral H, Pratoto A, Gulo EF, Arrafi MR, Sibarani EI, et al. Indonesian bay leaf (Syzygium polyanthum Wight) extract as a natural additive for UV and red light-blocking polyvinyl alcohol films with enhanced mechanical properties. Case Studies in

Chemical and Environmental Engineering 2025;11:101237. https://doi.org/10.1016/j.cscee.2025.101237.
[28] Rahmadiawan D, Akmal, Abral H, Azka MA, Sapuan SM, Kadriadi, et al. Solvent-selective extraction of Syzygium polyanthum bioactives for tailored polyvinyl alcohol composites: A lignocellulose-derived approach toward biorefinery-based functional materials. Biomass Bioenergy 2026;204:108467. https://doi.org/10.1016/j.biombioe.2025.108467.
[29] Buasri A, Poosri P, Ninprasert P, Niyasom A, Loryuenyong V. Preparation and Characterization of Plant Extract-Loaded PVA/GO Nanocomposite Films for Food Packaging. The 4th International Electronic Conference on Applied Sciences, Basel Switzerland: MDPI; 2023, p. 144. https://doi.org/10.3390/ASEC2023-15980.
[30] Mohamad EA, Shehata AM, Abobah AM, Kholief AT, Ahmed MA, Abdelhakeem ME, et al. Chitosan-based films blended with moringa leaves and MgO nanoparticles for application in active food packaging. Int J Biol Macromol 2023;253:127045. https://doi.org/10.1016/j.ijbiomac.2023.127045.
[31] Bhat VG, Narasagoudr SS, Masti SP, Chougale RB, Vantamuri AB, Kasai D. Development and evaluation of Moringa extract incorporated Chitosan/Guar gum/Poly (vinyl alcohol) active films for food packaging applications. Int J Biol Macromol 2022;200:50–60. https://doi.org/10.1016/j.ijbiomac.2021.12.116.
[32] Nam S, French AD, Condon BD, Concha M. Segal crystallinity index revisited by the simulation of X-ray diffraction patterns of cotton cellulose Iβ and cellulose II. Carbohydr Polym 2016;135:1–9. https://doi.org/10.1016/j.carbpol.2015.08.035.
[33] Prova FS, Toda A, Fukao K, Konishi T, Taguchi K. Influence of cellulose nanofibers on the crystallization behavior of polyvinyl alcohol nanocomposites. Polymer (Guildf) 2026;359:130270. https://doi.org/10.1016/j.polymer.2026.130270.
[34] Miao W, Wang J, Li G, Liu S, Luo X. Superior thermal stability of PVA/cellulose composite membranes for lithium-ion battery separators prepared by impregnation method with noncovalent cross-linking of intermolecular multiple hydrogen-bonds. J Energy Storage 2023;66:107353. https://doi.org/10.1016/j.est.2023.107353.
[35] Yeşilyurt A. Development and Characterization of PVA/KGM-Based Bioactive Films Incorporating Natural Extracts and Thyme Oil. Polymers (Basel) 2025;17:2425. https://doi.org/10.3390/polym17172425.
[36] Nayak B, Jain P, Kumar L, Mishra AA, Gaikwad KK. UV blocking edible films based on corn starch/moringa gum incorporated with pine cone extract for sustainable food packaging. Int J Biol Macromol 2024;267:131545. https://doi.org/10.1016/j.ijbiomac.2024.131545.
[37] Li Y, Chen Y, Wu Q, Huang J, Zhao Y, Li Q, et al. Improved Hydrophobic, UV Barrier and Antibacterial Properties of Multifunctional PVA Nanocomposite Films Reinforced with Modified Lignin Contained Cellulose Nanofibers. Polymers (Basel) 2022;14:1705. https://doi.org/10.3390/polym14091705.
[38] Zhang X, Liu W, Yang D, Qiu X. Biomimetic Supertough and Strong Biodegradable Polymeric Materials with Improved Thermal Properties and Excellent UV-Blocking Performance. Adv Funct Mater 2019;29. https://doi.org/10.1002/adfm.201806912.
[39] Haas HC, Husek H, Taylor LD. On the ultraviolet absorption spectrum of polyvinyl alcohol. J Polym Sci A 1963;1:1215–26. https://doi.org/10.1002/pol.1963.100010412.
[40] Zhang Y, Jiang W. Effective strategies to enhance ultraviolet barrier ability in biodegradable polymer-based films/coatings for fruit and vegetable packaging. Trends Food Sci Technol 2023;139:104139. https://doi.org/10.1016/j.tifs.2023.104139.
[41] Widyaningrum BA, Amanda P, Pramasari DA, Ningrum RS, Kusumaningrum WB, Kurniawan YD, et al. Preparation of a Conductive Cellulose Nanofiber-reinforced PVA Composite Film with Silver Nanowires Loading. Nano-Structures & Nano-Objects 2022;31:100904. https://doi.org/10.1016/j.nanoso.2022.100904.

[42] Ezati P, Khan A, Priyadarshi R, Bhattacharya T, Tammina SK, Rhim J-W. Biopolymer-based UV protection functional films for food packaging. Food Hydrocoll 2023;142:108771. https://doi.org/10.1016/j.foodhyd.2023.108771.
[43] Abral H, Ikhsan M, Rahmadiawan D, Handayani D, Sandrawati N, Sugiarti E, et al. Anti-UV, antibacterial, strong, and high thermal resistant polyvinyl alcohol/Uncaria gambir extract biocomposite film. Journal of Materials Research and Technology 2022;17:2193–202. https://doi.org/10.1016/j.jmrt.2022.01.120.
[44] Ji X, Guo J, Guan F, Liu Y, Yang Q, Zhang X, et al. Preparation of Electrospun Polyvinyl Alcohol/Nanocellulose Composite Film and Evaluation of Its Biomedical Performance. Gels 2021;7:223. https://doi.org/10.3390/gels7040223.
[45] Qin J, Huang X, Xu Q, Jin L. Active polyvinyl alcohol films with enhanced strength, antioxidant and antibacterial properties by incorporating nanocellulose and tannin. Int J Biol Macromol 2024;283:137873. https://doi.org/10.1016/j.ijbiomac.2024.137873.